Inorganic Chemistry

Article

Synthesis of the Novel [W₃PdS₄H₃(dmpe)₃(CO)]⁺ Cubane Cluster and Kinetic Studies on the Substitution of Coordinated Hydrides in Acidic Media

Andrés G. Algarra,[†] Manuel G. Basallote,*[,†] Marta Feliz,[‡] M. Jesús Fernández-Trujillo,[†] Eva Guillamón,[‡] Rosa Llusar,*[,‡] and Cristian Vicent[‡]

Departamento de Ciencia de los Materiales e Ingeniería Metalúrgica y Química Inorgánica, Facultad de Ciencias, Universidad de Cádiz, Apartado 40, Puerto Real, 11510 Cádiz, Spain, and Departament de Ciències Experimentals, Universitat Jaume I, Campus de Riu Sec, Box 224, 12071 Castelló, Spain

Reaction of the incomplete cuboidal [W₃S₄H₃(dmpe)₃]⁺ cluster with a Pd(0) complex under a CO atmosphere produces a rare example of a heterodimetallic hydrido cluster of formula [W₃PdS₄H₃(dmpe)₃(CO)]⁺ ([**1**]⁺). There are not significant changes in the W–W bond lengths on going from the trinuclear to the tetranuclear cluster. The average W–W and W–Pd bond distances of 2.769[10] and 2.90[2] Å, respectively, are consistent with the presence of single bonds between metal atoms. The heterodimetallic [**1**]⁺ complex is easier to oxidize and more difficult to reduce than its trinuclear precursor, which reflects the electron-donating capability of the Pd(CO) fragment. However, mechanistic studies on the reaction of [**1**]⁺ with acids show a lower basicity for this complex in comparison with that of its trinuclear precursor, so there is a major electron-density rearrangement within the cluster core upon Pd(CO) coordination. This rearrangement is also reflected in an unusual expansion of the sulfur tetrahedron within the W₃PdS₄ core with the concomitant elongation of the W–S bond distances by 0.04 Å with respect to the analogous bond lengths in the trinuclear precursor. For those thermodynamically favored proton-transfer processes, the reaction mechanism of [**1**]⁺ with acids is quite similar to that observed for the incomplete trinuclear cluster, with only small changes in the rate constants. The reaction of [**1**]⁺ with HCl in acetonitrile/water mixtures produces [W₃PdS₄Cl₃(dmpe)₃(CO)]⁺ ([**2**]⁺) in two kinetically distinguishable steps. Proton transfer occurs in the initial step, in which the W–H bonds are attacked by the acid to yield dihydrogen-bonded adducts that are further attacked by an acetonitrile molecule to give [W₃PdS₄(CH₃CN)₃(dmpe)₃(CO)]⁴⁺ and dihydrogen. The nature of processes involved in the second step are not well-understood with the present data, although it is very likely that these correspond to some secondary processes. In the third resolved step, the coordinated CH₃CN ligands in [W₃PdS₄(CH₃CN)₃(dmpe)₃(CO)]⁴⁺ are substituted by Cl⁻ to afford the final [**2**]⁺ product. No reaction is observed between [**1**]⁺ and HCl in neat acetonitrile, whereas the product of the reaction of [**1**]⁺ with HBF₄ or Hpts (pts⁻ = *p*-toluenesulfonate) in this solvent is [W₃PdS₄(CH₃CN)₃(dmpe)₃(CO)]⁴⁺. The reaction occurs in a single kinetic step with a first- (Hpts) or second-order (HBF₄) dependence with respect to the acid. The first- and second-order acid dependences can be interpreted through the initial formation of dihydrogen adducts with one or two acid molecules, respectively.

Introduction

Heterodimetallic sulfide clusters of molybdenum and tungsten are nowadays easily accessible through building block strategies starting from incomplete cuboidal M₃(μ₃-S)(μ-S)₃ (M= Mo, W) clusters.[1–5] Cubane type metal sulfide

* To whom correspondence should be addressed. Fax: 34 964 728066 (R.L.). Tel: 34 964 728086 (R.L.). E-mail: llusar@exp.uji.es (R.L); manuel.basallote@uca.es (M.G.B.).
† Universidad de Cádiz.
‡ Universitat Jaume I.

(1) Shibahara, T.; Yamamoto, T.; Sakane, G. *Chem. Lett.* **1994**, 1231.
(2) Hidai, M.; Kuwata, S.; Mizobe, Y. *Acc. Chem. Res.* **2000**, *33*, 46.
(3) Hernandez-Molina, R.; Sokolov, M. N.; Sykes, A. G. *Acc. Chem. Res.* **2001**, *34*, 223.
(4) Sakane, G.; Shibahara, T. *Inorg. Synth.* **2002**, *33*, 150.
(5) Akashi, H.; Isobe, K.; Shibahara, T. *Inorg. Chem.* **2005**, *44*, 3494.

complexes have been extensively used as models for the active sites of metalloenzymes and industrial metal sulfide catalysts.[6] Incorporation of palladium into the $M_3(\mu_3\text{-}S)(\mu\text{-}S)_3$ unit has allowed for the preparation of tetrametallic M_3PdS_4 complexes, which exhibit a remarkable catalytic activity for the addition of alcohols and carboxylic acids to electron-deficient alkynes.[7−9] The interest of transition-metal hydrides in catalysis combined with the catalytic activity of these M_3PdS_4 cubane complexes has encouraged us to study the incorporation of Pd into W_3S_4 cluster hydrides.

Trinuclear hydride clusters of group six metals have been isolated only for tungsten within the complex series of formula $[W_3Q_4H_3(\text{diphosphine})_3]^+$ (Q = S, Se; diphos = dmpe, dppe).[10,11] The hydride ligands in these compounds occupy terminal positions, in contrast with the most-common edge-bridging coordination mode found in other trinuclear cluster chalcogenides.[12,13] Up to date, there is only one example of heterodimetallic cubane type sulfido clusters containing hydride ligands, namely the $[Mo_3RuS_4Cp^*_3H_2\text{-}(PPh_3)]^+$ cation, in which the ruthenium is coordinated to two hydrides and one phosphine.[14] The ruthenium atom in this cluster is quite unique, binding hydrogen reversibly under mild conditions. In addition, this Mo_3RuS_4 hydride cluster is effective for the N−N bond cleavage of hydrazines to produce ammonia and nitrogen.[15]

In this work, we report the synthesis, structure, and electrochemical properties of the $[W_3PdS_4H_3(dmpe)_3(CO)]^+$ ($[\mathbf{1}]^+$) hydrido cubane. This complex is the second example of a cubane type sulfido cluster containing hydride ligands. However, in contrast with the $[Mo_3RuS_4Cp^*_3H_2(PPh_3)]^+$ complex, in which the heterometal bears both hydride ligands, each hydride ligand in $[W_3PdS_4H_3(dmpe)_3(CO)]^+$ occupies a terminal position on each tungsten atom, as found in its trinuclear $[W_3S_4H_3(dmpe)_3]^+$ precursor. The properties of this last trinuclear cluster, air stability and solubility in a wide variety of solvents, make it an excellent substrate for investigating the mechanism of protonation of hydride complexes. Thus, the terminal hydrides in $[W_3Q_4H_3(dmpe)_3]^+$ undergo acid-promoted substitution reactions through the formation of dihydrogen-bonded adducts, with the kinetics and mechanism showing a strong dependence on the

coordinating capability of the solvent.[16−18] The tetranuclear cluster shares properties regarding stability and solubility with its trinuclear precursor; as a result of that, it provides a unique opportunity for studying the effect that the incorporation of a second metal has on the basicity and protonation mechanism of the tungsten-coordinated hydrides in these W_3PdS_4 cubane type clusters.

Experimental Section

General Remarks. $[W_3S_4H_3(dmpe)_3][PF_6]$ was prepared according to literature methods.[10] $[Pd_2(dba)_3]$ (dba = dibenzylidenacetone) was purchased from Strem Chemicals. Solvents for synthesis and electrochemical measurements were dried and degassed by standard methods before use.

Physical Measurements. Elemental analyses were performed on an EA 1108 CHNS microanalyzer at the Universidad de La Laguna. $^{31}P\{^1H\}$ NMR spectra were recorded on a Varian MERCURY 300 MHz instrument and were referenced to external 85% H_3PO_4. ^1H, $^{13}C\{^1H\}$, and $^1H−^{13}C$ gHSQC spectra were recorded on a Varian INOVA 500 MHz instrument using CD_2Cl_2 or acetone-d_6 as solvent. Chemical shifts are reported in parts per million from tetramethylsilane with the solvent resonance as the internal standard. IR spectra were recorded on a Perkin−Elmer System 2000 FT-IR instrument using KBr pellets. Signal intensities are denoted as s = strong, m = medium, and w = weak. Electronic absorption spectra were obtained on a Perkin−Elmer Lambda-19 spectrophotometer in dichloromethane. Electrospray mass spectra were recorded with a Quattro LC (quadrupole−hexapole−quadrupole) mass spectrometer with an orthogonal Z-spray electrospray interface (Micromass, Manchester, U.K.). The cone voltage was set at 20 V unless otherwise stated, using CH_3CN as the mobile-phase solvent. Nitrogen was employed as the drying and nebulizing gas. Isotope experimental patterns were compared with theoretical patterns obtained using the MassLynx 4.0 program.[19] Cyclic voltammetry experiments were performed with an Echochemie Pgstat 20 electrochemical analyzer. All measurements were carried out at room temperature with a conventional three-electrode configuration consisting of platinum working and auxiliary electrodes and an Ag/AgCl reference electrode containing aqueous 3 M KCl. Dichloromethane was used as the solvent in all experiments. The supporting electrolyte was 0.1 mol dm⁻³ tetrabutylammonium hexafluorophosphate. $E_{1/2}$ values were determined as being $^1\!/_2(E_a + E_c)$, where E_a and E_c are the anodic and cathodic peak potentials, respectively. All potentials reported are not corrected for the junction potential. Potentials reported versus SCE have been referenced to Ag/AgCl as $E_{1/2}(\text{SCE}) − E_{1/2}(\text{Ag/AgCl}) = 0.04$ V on the basis of the values provided for the Fc⁺/Fc couple.

Synthesis. $[W_3PdS_4H_3(dmpe)_3(CO)][PF_6]$ ($[\mathbf{1}][PF_6]$). To a pink solution of $[W_3S_4H_3(dmpe)_3][PF_6]$ (0.2 g, 0.16 mmol) in CH_2Cl_2 (30 cm³) was added an excess of $[Pd_2(dba)_3]$ (0.080 g, 0.09 mmol) under nitrogen, and the color changed to red. After CO was bubbled through the solution for 30 min at room temperature, the reaction mixture was stirred for a day under a CO atmosphere and filtered. The resulting solution was then precipitated with Et₂O, and the solid recrystallized from CH_2Cl_2/Et_2O mixtures to afford a red micro-

(6) Brorson, M.; King, J. D.; Kiriakidou, K.; Prestopino, F.; Nordlander, E. In *Metal Clusters in Chemistry*; Braustein, P., Oro, L. A., Raithby, P. R., Eds.; Wiley-VCH: Weinheim, 1999; Vol. 2.

(7) Murata, T.; Mizobe, Y.; Gao, H.; Ishii, Y.; Wakabayashi, T.; Nakano, F.; Tanase, T.; Yano, S.; Hidai, M.; Echizen, I.; Nanikawa, H.; Motomura, S. *J. Am. Chem. Soc.* **1994**, *116*, 3389.

(8) Wakabayashi, T.; Ishii, Y.; Murata, T.; Mizobe, Y.; Hidai, M. *Tetrahedron Lett.* **1995**, *36*, 5585.

(9) Wakabayskhi, T.; Ishii, Y.; Ishikawa, K.; Hidai, M. *Angew. Chem., Int. Ed.* **1996**, *35*, 2123.

(10) Cotton, F. A.; Llusar, R.; Eagle, C. T. *J. Am. Chem. Soc.* **1989**, *111*, 4332.

(11) Estevan, F.; Feliz, M.; Llusar, R.; Mata, J. A.; Uriel, S. *Polyhedron* **2001**, *20*, 527.

(12) Bright, T. A.; Jones, R. A.; Koschmieder, S. U.; Nunn, C. N. *Inorg. Chem.* **1988**, *27*, 3819.

(13) Kuwata, S.; Andou, M.; Hashizume, K.; Mizobe, Y.; Hidai, M. *Organometallics* **1998**, *17*, 3429.

(14) Takei, I.; Suzuki, K.; Enta, Y.; Dohki, K.; Suzuki, T.; Mizobe, Y.; Hidai, M. *Organometallics* **2003**, *22*, 1790.

(15) Takei, L.; Dohki, K.; Kobayashi, K.; Suzuki, T.; Hidai, M. *Inorg. Chem.* **2005**, *44*, 3768.

(16) Basallote, M. G.; Estevan, F.; Feliz, M.; Fernandez-Trujillo, M. J.; Hoyos, D. A.; Llusar, R.; Uriel, S.; Vicent, C. *Dalton Trans.* **2004**, 530.

(17) Basallote, M. G.; Feliz, M.; Fernandez-Trujillo, M. J.; Llusar, R.; Safont, V. S.; Uriel, S. *Chem.−Eur. J.* **2004**, *10*, 1463.

(18) Algarra, A. G.; Basallote, M. G.; Feliz, M.; Fernandez-Trujillo, M. J.; Llusar, R.; Safont, V. S. *Chem.−Eur. J.* **2006**, *12*, 1413.

(19) *MASSLYNX*, 4.0 ed.; Micromass Ltd.: Manchester, U.K., 2005.

crystalline product characterized as $[W_3PdS_4H_3(dmpe)_3(CO)][PF_6]$ ($[\mathbf{1}][PF_6]$) (0.199 g, 90%). Calcd for $C_{19}H_{51}F_6OP_7PdS_4W_3$: S, 9.08; C, 16.15; H, 3.64. Found: S, 9.02; C, 16.54; H, 3.88. λ_{max} (nm): 515 (sh), 463, 392. IR (cm^{-1}): 2008 (s, CO), 1741 (s, W−H), 1418 (s), 1299 (m), 1285 (m), 1135 (m), 938 (i), 898 (m), 837 (s, P−F), 744 (m), 714 (m), 654 (m), 557 (s, P−F), 423 (w), 338 (w). $^{31}P\{^1H\}$ NMR: δ −143.44 (sept, $^1J(P-F) = 704.0$ Hz), −10.12 (d, $^2J(P-P) = 9.7$ Hz, $^1J(P-W) = 133.7$ Hz), 3.01 (d, $^2J(P-P) = 9.7$ Hz, $^1J(P-W) = 181.0$ Hz). ^1H NMR: δ −2.68 (3H hydride, dd, $^2J(P-H) = 46.0$ Hz, $^2J(P'-H) = 28.5$ Hz), 0.86 (9H, CH_3, d, $^2J(P-H) = 9.0$ Hz), 1.51 (3H, CH_2, m), 1.81 (9H, CH_3, d, $^2J(P-H) = 8.0$ Hz), 1.84 (3H, CH_2, m), 1.85 (9H, CH_3, d, $^2J(P-H) = 7.5$ Hz), 1.99 (9H, CH_3, d, $^2J(P-H) = 9.0$ Hz), 2.01 (3H, CH_2, m), 2.40 (3H, CH_2, m,). $^{13}C\{^1H\}$ NMR: δ 14.71 (CH_3, d, $^1J(C-P) = 25.3$ Hz), 19.06 (CH_3, d, $^1J(C-P) = 24.5$ Hz), 21.19 (CH_3, d, $^1J(C-P) = 30.2$ Hz), 22.54 (CH_3, d, $^1J(C-P) = 29.3$ Hz), 28.50 (CH_2, dd, $^1J(C-P) = 21.8$ Hz, $^2J(C-P) = 3.0$ Hz), 29.40 (CH_2, dd, $^1J(C-P) = 25.7$ Hz, $^2J(C-P) = 4.0$ Hz). Electrospray-MS (cone voltage 65 V): m/z 1268 (M$^+$), 1240 (M$^+$ − CO).

$[W_3PdS_4Cl_3(dmpe)_3(CO)][PF_6]$ ($[\mathbf{2}][PF_6]$). To a red solution of $[W_3PdS_4H_3(dmpe)_3(CO)][PF_6]$ ($[\mathbf{1}][PF_6]$) (0.07 g, 0.05 mmol) in 5 cm^3 of CH$_3$CN was added aqueous HCl (3 cm^3, 0.1 M), and the resulting mixture was stirred for 10 min. Partial evaporation of the solvent (ca. 4 cm^3) precipitates the desired product as a red-brown microcrystalline solid, which was filtered; washed with water, 2-propanol, and diethyl ether; and dried to afford $[W_3PdS_4Cl_3(dmpe)_3(CO)][PF_6]$ ($[\mathbf{2}][PF_6]$) (0.065 g, 87%). Calcd for $C_{19}H_{48}Cl_3F_6OP_7PdS_4W_3$: S, 8.45; C, 15.05; H, 3.20. Found: S, 8.41; C, 15.04; H, 3.18. λ_{max} (nm): 549, 413 (sh), 385. IR (cm^{-1}): 2043 (s, CO), 1741 (s, W−H), 1416 (s), 1302 (m), 1286 (m), 1136 (m), 951 (s), 940 (s), 899 (m), 832 (s, P−F), 747 (m), 710 (m), 650 (m), 557 (s, P−F), 438 (w), 415 (w), 336 (w). $^{31}P\{^1H\}$ NMR: δ −143.44 (sept, $^1J(P-F) = 704.0$ Hz), −0.50 (s, $^1J(P-W) = 184.4$ Hz), −4.12 (s, $^1J(P-W) = 173.5$ Hz); ^1H NMR: δ 1.26 (9H, CH_3, d, $^2J(P-H) = 9.5$ Hz), 1.72 (9H, CH_3, $^2J(P-H) = 9.5$ Hz), 1.76 (9H, CH_3, d, $^2J(P-H) = 11.0$ Hz), 1.81 (3H, CH_2, m), 1.95 (3H, CH_2, m), 2.01 (9H, CH_3, $^2J(P-H) = 10.0$ Hz), 2.21 (3H, CH_2, m), 2.55 (3H, CH_2, m). $^{13}C\{^1H\}$ NMR: δ 12.27 (CH_3, d, $^1J(C-P) = 29.0$ Hz), 12.88 (CH_3, d, $^1J(C-P) = 26.7$ Hz), 14.61 (CH_3, d, $^1J(C-P) = 32.8$ Hz), 19.99 (CH_3, d, $^1J(C-P) = 31.3$ Hz), 27.40 (CH_2, dd, $^1J(C-P) = 27.5$ Hz, $^2J(C-P) = 8.9$ Hz), 28.13 (CH_2, dd, $^1J(C-P) = 23.4$ Hz, $^2J(C-P) = 9.1$ Hz). Electrospray-MS (cone voltage 65 V): m/z 1370 (M$^+$), 1342 (M$^+$ − CO).

Kinetic Experiments. The kinetics of the reaction of the $[\mathbf{1}]^+$ cluster with acids was studied at 25.0 °C using an Applied Photophysics SX17MV stopped-flow instrument provided with a PDA1 diode-array detector, and the results were analyzed with the SPECFIT program.[20] The experiments were carried out using either CH$_3$CN−H$_2$O (1:1 v/v) or neat CH$_3$CN as solvent. Because solutions of $[\mathbf{1}][PF_6]$ in CH$_3$CN−H$_2$O are not stable, the kinetic experiments in this mixture of solvents were carried out by mixing in the stopped-flow instrument solutions of this compound in neat CH$_3$CN with aqueous solutions of the acid. Although this led to an increase in the dead time for the kinetic experiments in CH$_3$CN−H$_2$O mixtures, it did not affect the results; this is because no reaction occurs to a significant extent during the mixing time, so the data could be always fitted satisfactorily using the appropriate model (single or consecutive exponentials) and yielded reproducible values of the rate constants. The solutions of acid contained in all cases the amount of Et$_4$NBF$_4$ or Li(pts) required to achieve a constant ionic strength of 0.1 mol dm^{-3} in the solution arriving in the

stopped-flow cell. The concentration of acid was determined in each case by titration with a previously standardized KOH solution; for the acid solutions in CH$_3$CN, the titrations were carried out after diluting an aliquot (1−2 cm^3) with water (50 cm^3). For the kinetic experiments in neat CH$_3$CN, HCl was generated by reaction of ClSiMe$_3$ with MeOH.

X-ray Studies. Replacement of the PF$_6^-$ anion in cluster $[\mathbf{1}][PF_6]$ was done by adding an excess of Na[BPh$_4$] to a methanol solution of $[\mathbf{1}]^+$ that precipitates the desired tetraphenylborate salt. Suitable crystals for X-ray studies for compound $[\mathbf{1}][BPh_4]$ were grown by slow diffusion of toluene into a sample solution in CH$_2$Cl$_2$. The crystals are air-stable and were mounted on the tip of a glass fiber with the use of epoxy cement. X-ray diffraction experiments were carried out on a Bruker SMART CCD diffractometer using Mo−Kα radiation ($\lambda = 0.71073$ Å) at room temperature. The data were collected with a frame width of 0.3° in ω and a counting time of 10 s per frame. The diffraction frames were integrated using the SAINT package and corrected for absorption with SADABS.[21,22] The structures were solved by direct methods and refined by the full-matrix method on the basis of F^2 using the SHELXTL software package.[23] The structure of $[\mathbf{1}][BPh_4]$ was successfully solved in the monoclinic $C2/c$ space group. All non-hydrogen atoms both in the cluster and the tetraphenylborate anion were refined anisotropically. The positions of all hydrogen atoms were generated geometrically, assigned isotropic thermal parameters, and allowed to ride on their respective parent carbon atoms. Crystal data for $[\mathbf{1}][BPh_4]$: $BC_{43}H_{71}F_6OP_6PdS_4W_3$, M = 1586.82, monoclinic, space group $C2/c$, $a = 32.037(3)$ Å, $b = 21.782(2)$ Å, $c = 22.351(2)$ Å, $\beta = 134.204(2)°$, $V = 11181.1(18)$ Å^3, $T = 293$ K, $Z = 8$, $\rho_{calcd} = 1.885$ g/cm^3, $\mu(MoK\alpha) = 6.820$ mm^{-1}. Number of reflections collected/unique = 38 487/12 821 (R$_{int}$ = 0.0928). Final refinement converged with R$_1$ = 0.0489 for 7305 reflections with $F_0 \geq 4\sigma(F_0)$ and wR$_2$ = 0.1162 for all reflections, GOF = 1.028, max/min residual electron density 1.624/−1.384 e Å^{-3}.

Results and Discussion

Synthesis and Redox Properties. Trinuclear M$_3(\mu_3$-S)-$(\mu$-S)$_3$ (M = Mo, W) cubane type clusters have been widely used as metalloligands toward other transition metals to produce a large variety of heterodimetallic M$_3$M′$(\mu_3$-S)$_4$ complexes.[24] This chemistry has been mainly developed in water; the major advances are found for molybdenum clusters, for which the heterometals incorporated range from group 6 to group 15 elements.[25,26] For tungsten, the number of heterometals is more restricted, namely In, Ge, Sn, Mo, Re, Ni, Pt, and Cu; this fact has been attributed to the greater difficulty in reducing tungsten compared to molybdenum. The formation of the $[M_3PdS_4]^{n+}$ aquo ion has only been shown for molybdenum.[27] Recently, a nonaqueous chemistry has emerged parallel to the M$_3$M′S$_4$ chemistry developed in

(20) Binstead, R. A.; Jung, B.; Zuberbühler, A. D. *SPECFIT*; Spectrum Software Associates: Chapel Hill, NC, 2000.

(21) *SAINT*, version 6.2; Bruker Analytical X-ray Systems: Madison, WI, 2001.
(22) Sheldrick, G. M. *SADABS Empirical Absorption Program*; University of Göttingen: Göttingen, Germany, 1996.
(23) Sheldrick, G. M. *SHELXTL*, version 5.1; Bruker Analytical X-ray Systems: Madison, WI, 1997.
(24) Llusar, R.; Uriel, S. *Eur. J. Inorg. Chem.* **2003**, 1271.
(25) Shibahara, T. *Coord. Chem. Rev.* **1993**, *123*, 73.
(26) Hernandez-Molina, R.; Sykes, A. G. *J. Chem. Soc., Dalton Trans.* **1999**, 3137.
(27) Fedin, V. P.; Seo, M. S.; Saysell, D. M.; Dybtsev, D. N.; Elsegood, M. R. J.; Clegg, W.; Sykes, A. G. *Dalton Trans.* **2002**, 138.
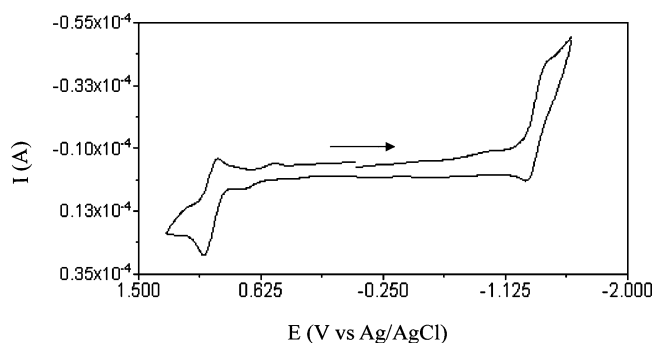
Figure 1. Cyclic voltammogram of [W₃PdS₄Cl₃(dmpe)₃(CO)][PF₆] ([**2**][PF₆]) registered at 250 mV/s.

Figure 2. ORTEP representation of the cationic cluster [W₃PdS₄H₃-(dmpe)₃(CO)]⁺ ([**1**]⁺).

water. Typical precursors used are the cyclopentadienyl [M₃S₄(η⁵-Cp′)₃]⁺ clusters and the diphosphine [M₃S₄X₃-(diphosphine)₃]⁺ cations. In the case of palladium, the synthesis of [W₃PdS₄Cp′₃(PPh₃)]⁺ in 92% yield starting from [W₃S₄(η⁵-Cp′)₃]⁺ and [Pd₂(dba)₃] in the presence of PPh₃ has been reported.[28] In a similar way, reaction of the trinuclear [W₃S₄H₃(dmpe)₃]⁺ cation with [Pd₂(dba)₃] followed by CO treatment results in the high-yield formation of the heterodimetallic [W₃PdS₄H₃(dmpe)₃(CO)]⁺ ([**1**]⁺) cluster hydride. Complex [**1**]⁺ reacts with HCl with substitution of the terminal hydride ligands by chloride to afford [W₃PdS₄Cl₃(dmpe)₃(CO)]⁺ ([**2**]⁺) in 87% yields. As found for their trinuclear [W₃S₄H₃(dmpe)₃]⁺ precursor, the reaction is acid-promoted and no ligand replacement is observed with halide salts in the absence of acids. Details on the reaction mechanism of [**1**]⁺ with acids are given in a later section.

The cyclic voltammogram of [**2**]⁺ is represented in Figure 1, with one irreversible reduction wave at − 1.31 V and one quasireversible oxidation process at + 1.00 V. A similar redox behavior has been seen for [W₃PdS₄(η⁵-Cp′)₃(PPh₃)]⁺, with a chemically reversible one-electron reduction ($E_{1/2}^{+/0}$ = −1.35 V) and a two-electron oxidation ($E_{1/2}$ = 0.52 V) followed by a first-order reversible chemical reaction. By analogy, we can tentatively identify the two redox waves seen for [**2**]⁺ on the basis of the assignment for [W₃PdS₄-(η⁵-Cp′)₃(PPh₃)]⁺, although confirmation of this hypothesis is out of the scope of this work.[28] In the case of [**1**]⁺, no reduction wave can be seen because of the closeness of the process to the solvent discharge. It is well-known that trinuclear [W₃S₄H₃(diphosphine)₃]⁺ hydride complexes are more difficult to reduce than their corresponding halides.[11] On the other hand, [W₃PdS₄H₃(dmpe)₃(CO)]⁺ ([**1**]⁺) is easier to oxidize than [**2**]⁺, with a half potential value $E_{1/2}$ = 0.53 V, similar to that measured for [W₃PdS₄(η⁵-Cp′)₃(PPh₃)]⁺. For the oxidation wave in [**1**]⁺ and [**2**]⁺, we observed a decrease in the $i_{p,c}/i_{p,a}$ ratio with the scan rate, in agreement with a chemical process following the electron removal.

The insertion of the Pd(PPh₃) fragment into the [W₃S₄-(η⁵-Cp′)₃]⁺ cluster produces a cathodic shift of 230 mV in the reduction potential and an anodic shift of ca. 1 V in the potential of the oxidation wave. In our system, the same tendency is observed, although the shifts upon Pd(CO)
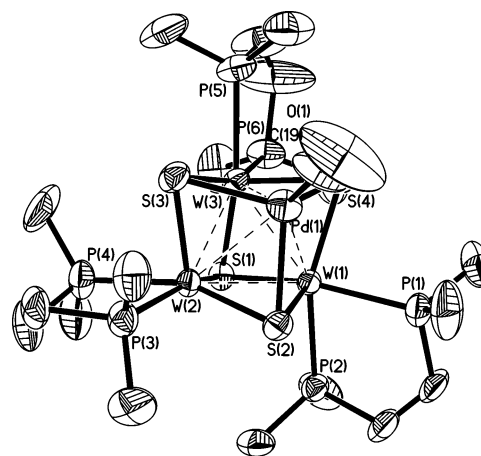
(28) Herbst, K.; Zanello, P.; Corsini, M.; D'Amelio, N.; Dahlenburg, L.; Brorson, M. *Inorg. Chem.* **2003**, *42*, 974.

incorporation cannot be quantified, because neither the reduction wave for [**1**]⁺ nor the oxidation process for [W₃S₄H₃(dmpe)₃]⁺ is observed within the solvent window. As a consequence, coordination of the palladium fragment to the cuboidal W₃S₄ cluster unit exerts an electron-donating effect. At this point, it is interesting to analyze how this effect influences the reactivity of the hydride ligands coordinated to the tungsten atoms in these W₃PdS₄ clusters. Although one may expect a higher basicity of the hydride ligands upon Pd incorporation, the opposite effect is observed (vide infra), so the additional electron density is not localized in the W−H bond.

Structure. Compound [**1**][BPh₄] crystallizes in the monoclinic *C*2/*c* space group without a crystallographically imposed *C₃* symmetry; however, the small differences in the intermetallic W−W distances are indicative of an effective *C₃* symmetry, in agreement with the presence of two different resonance signals in the ³¹P{¹H} NMR spectra. Figure 2 shows an ORTEP drawing of the [**1**]⁺ cluster cation, together with the atom-numbering scheme. The metal cluster core consists of a slightly distorted tetrahedral arrangement of one palladium and three tungsten atoms. Each tetrahedral face is capped by a μ₃-coordinated sulfide ligand, thus generating a cubane-like structure. The coordination sphere on each tungsten atom is essentially octahedral, whereas the palladium atom appears in a tetrahedral environment. For the metal site W(1) (also applicable to W(2) and W(3)), there are two phosphorus atoms, P(1) and P(2), located trans to μ₃-S(1) and μ₃-S(4), respectively, and a vacant position associated with the hydride ligand trans to the μ₃-S(2) bridging ligand. The existence of three hydride ligands, one on each W atom, has been fully supported by ¹H and ³¹P NMR spectroscopy. The ¹H spectra in the hydride region show a doublet of doublets centered at −2.68 ppm, consistent with three equivalent hydrides coupled with the two nonequivalent phosphorus atoms bonded to the same metal with $^2J_{PH}$ = 46.0 and 28.5 Hz. The ³¹P NMR spectrum registered when selective decoupling of all but the hydridic hydrogen nuclei shows a splitting of the signals with $^2J_{PH}$ coupling constants of 45.4 and 27.3 Hz. These values agree within the experimental error with those measured from the ¹H

Table 1. Selected Average Bond Distances (Å) for Compounds [W₃PdS₄H₃(dmpe)₃(CO)][BPh₄] ([**1**][BPh₄]), [W₃S₄H₃(dmpe)₃][BPh₄], and [W₃PdS₄Cp′₃(PPh₃)][Pts]ᵃ

bond	[**1**][BPh₄]	[W₃S₄H₃(dmpe)₃]-[BPh₄][10]	[W₃PdS₄Cp′(PPh₃))-[pts][28]
W−W	2.769[10]	2.751[4]	2.805[8]
W−Pd	2.90[2]		2.910[9]
Pd−(μ_3-S)	2.472[9]		2.403[5]
W−(μ_3-S)	2.370[6]	2.335[9]	2.326[6]

ᵃ Standard deviations for averaged values are given in brackets.

spectrum, confirming the presence of one hydrogen atom attached to each metal site.

The tetrahedral environment on the palladium Pd(1) is defined by three bridging sulfur atoms and one carbonyl neutral fragment. Table 1 shows the most-relevant bond distances within the cluster unit in [**1**][BPh₄] together with those found for its trinuclear precursor [W₃S₄H₃(dmpe)₃]-[BPh₄].

The average W−W and W−Pd bond distances of 2.769[10] and 2.90[2] Å, respectively, are consistent with the presence of single bonds between metal atoms. There are no significant changes on the W−W bond lengths on going from [W₃S₄H₃-(dmpe)₃]⁺ to [W₃PdS₄H₃(dmpe)₃(CO)]⁺, whereas the W−S bond distance is elongated by 0.04 Å upon incorporation of the Pd(CO) fragment with a Pd−S distance of 2.472[9] Å. This complex shares structural features with the other structurally characterized W₃Pd cluster, namely [W₃PdS₄-(η⁵-Cp′)₃(PPh₃)]⁺, although in this case, the W−S bond lengths are considerably shorter, specifically 0.05 and 0.07 Å shorter for the W−S and Pd−S distances, respectively.[28] To visualize these differences, it is illustrative to look at the cuboidal W₃PdS₄ arrangement as two interpenetrated tetrahedrons, one formed by the W₃Pd unit and the other by the four capping sulfur atoms. Elongation of the W−S and Pd−S bond distances implies an expansion of the sulfur tetrahedron, also reflected by the opening of the S−W−S and S−Pd−S angles in the [**1**][BPh₄] cluster complex.

The CO ligand in [**1**]⁺ is coordinated to the Pd atom in an essentially linear Pd−C−O linkage with an angle of 174.8(16)°. The short Pd−C bond length of 1.926 (13) Å indicates a substantial π-back-donation from the Pd center to the CO ligand, also reflected in the low values of 2008 cm⁻¹ measured for ν(CO) infrared stretching frequencies. Although this ν(CO) frequency is higher than in known Pd(0) complexes, it is also significantly lower than in Pd²⁺ complexes.[29,30] Theoretical calculations suggest that the high CO stretching frequencies are not a consequence of the heterometal oxidation but rather are the result of the dual role of the heterometal d orbitals, which participate in the formation of the W−Pd bond and in back-bonding to the CO ligand.[31] Although oxidation state assignment in cubane type transition-metal complexes is a polemic task because of the strong electron delocalization, there is no question on
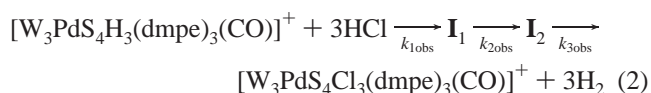
the basis of the electrochemical results regarding the electron-donor character of the Pd(CO) fragment upon coordination to the W₃S₄ unit.

In cluster [**1**]⁺, the extra electron density due to the heterometal incorporation results in the formation of three W−Pd bonds and three Pd−S bonds, in which the metal and sulfur orbitals participate in the formation of cluster orbitals delocalized over the entire W₃PdS₄ framework. The electron-donating capability of the Pd(CO) fragment is also reflected in the lengthening of the W−S bonds and expansion of the sulfur tetrahedron. However, this extra electron density surprisingly causes a decrease in the basicity of the hydride ligands coordinated to the tungsten atom; therefore, insertion of the heterometallic fragment to the W₃S₄ complex results in a redistribution of the electron density within the cluster core and the resulting effect on the W−H bond is a net withdrawal of electron density with regard to its trinuclear precursor. Thus, such diminution in the W−H electron density causes a decrease in the basicity of the coordinated hydrides, as will be seen in the next section.

Kinetics of the Reaction of Cluster [1]⁺ with Acids. The heterodimetallic cluster [W₃PdS₄H₃(dmpe)₃(CO)]⁺ ([**1**]⁺) reacts with acids (HCl) to form [W₃PdS₄Cl₃(dmpe)₃(CO)]⁺ ([**2**]⁺) in a way similar to that for the trinuclear [W₃Q₄H₃-(dmpe)₃]⁺ (Q = S, Se) cluster hydrides, whereas no reaction occurs when halide salts are used.[16,17] To analyze the influence of the heterometal on the acid-assisted substitution process represented in eq 1, we investigated its kinetics in the presence of coordinating solvents.

$$[W_3PdS_4H_3(dmpe)_3(CO)]^+ + 3HCl \rightarrow$$
$$[W_3PdS_4Cl_3(dmpe)_3(CO)]^+ + 3H_2 \ (1)$$
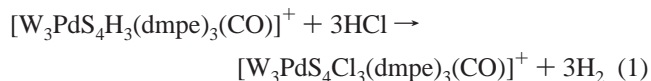
The kinetics of the reaction in eq 1 was studied in 0.1 mol dm⁻³ Et₄NBF₄ under pseudo-first-order conditions of acid excess in water−acetonitrile mixtures (1:1 v/v); kinetic features quite similar to those previously reported for the related complexes with incomplete cuboidal structure were observed.[17,18] A typical example of the spectral changes with time for the reaction in eq 1 is shown in Figure 3, where the inset plot is a representative kinetic trace extracted at 442.9 nm. These experimental data were satisfactorily fitted by using a model with three consecutive exponentials (eq 2), which yields the values of the rate constants for the three steps (k_{1obs}, k_{2obs}, and k_{3obs}) and the spectra of the starting complex, the reaction intermediates **I**₁ and **I**₂, and the final reaction product (Figure 4). The first-order dependence with respect to [**1**]⁺ was confirmed for all the steps by the lack of changes in the three observed rate constants when the complex concentration was changed.

$$[W_3PdS_4H_3(dmpe)_3(CO)]^+ + 3HCl \xrightarrow{k_{1obs}} I_1 \xrightarrow{k_{2obs}} I_2 \xrightarrow{k_{3obs}}$$
$$[W_3PdS_4Cl_3(dmpe)_3(CO)]^+ + 3H_2 \ (2)$$

The rate constants for the first step (k_{1obs}) change with the acid concentration according to eq 3 (see Figure 5), and the value derived for the corresponding second-order rate constant is $k_1 = 7.7 \pm 0.1$ dm³ mol⁻¹ s⁻¹. In contrast, the

(29) Yu, L.; Srinivas, G. N.; Schwartz, M. *J. Mol. Struct. (THEOCHEM)* **2003**, *625*, 215.
(30) Vicente, J.; Arcas, A.; Borrachero, M. V.; Tiripicchio, A.; Camellini, M. T. *Organometallics* **1991**, *10*, 3873.
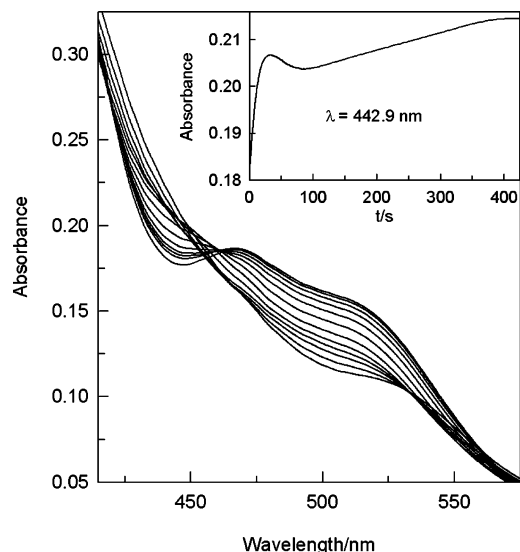(31) Bahn, C. S.; Tan, A.; Harris, S. *Inorg. Chem.* **1998**, *37*, 2770.

Figure 3. Typical spectral changes with time for the reaction of [**1**][PF₆] with HCl in CH₃CN−H₂O (1:1 v/v) at 25.0 °C. The inset represents the extracted kinetic trace at 442.9 nm.
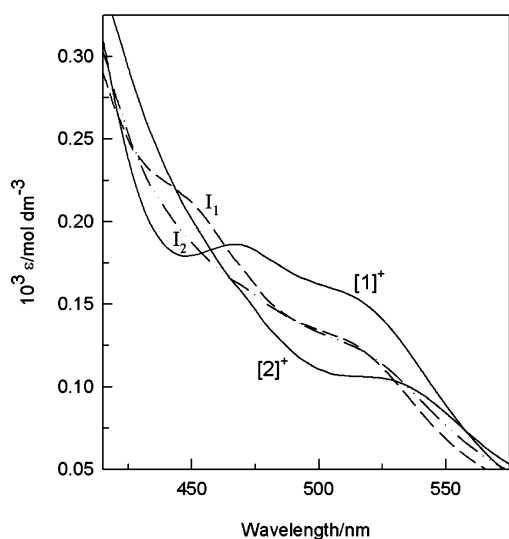

Figure 4. UV−vis spectra calculated for the starting complex [**1**]⁺, the reaction intermediates (**I₁**) and (**I₂**), and the final reaction product [**2**]⁺ for the reaction of [**1**]⁺ with HCl in CH₃CN−H2O (1:1 v/v).

rate constants for the last two steps (k_{2obs} and k_{3obs}) are independent of the concentration of acid: $k_2 = (5.6 \pm 0.6) \times 10^{-2}$ s⁻¹ and $k_3 = (1.0 \pm 0.2) \times 10^{-2}$ s⁻¹.

$$k_{1obs} = k_1[\text{H}^+] \tag{3}$$

To obtain more information about the effect of the Pd heterometal on the mechanism of the acid-assisted substitution in this kind of hydride clusters, we also attempted kinetic studies in neat CH₃CN. Surprisingly, no reaction between [**1**]⁺ and HCl occurs in this solvent, even when the acid concentration is quite high (up to ca. 0.5 mol dm⁻³). Because the corresponding trinuclear cluster [W₃S₄H₃(dmpe)₃]⁺ reacts with lower concentrations of HCl in similar conditions, it must be concluded that the presence of the Pd(CO) unit changes the thermodynamics of the process. The decrease in the basicity of the coordinated hydrides in [**1**]⁺ indicates that despite the electron-donating capability of the Pd(CO)
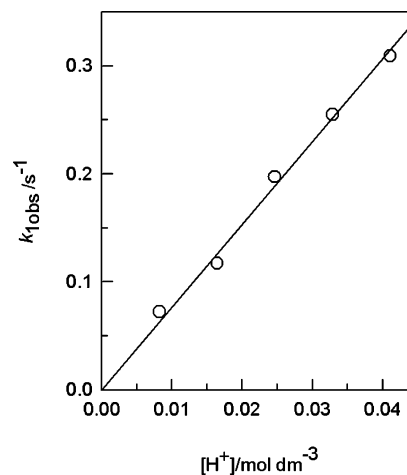

Figure 5. Plot of the observed rate constant for the first step in the reaction of [**1**]⁺ with HCl in CH₃CN−H₂O (1:1 v/v) mixtures (25.0 °C, 0.1 mol dm⁻³ Et₄NBF₄). The solid line corresponds to the overall fit of each set of data.
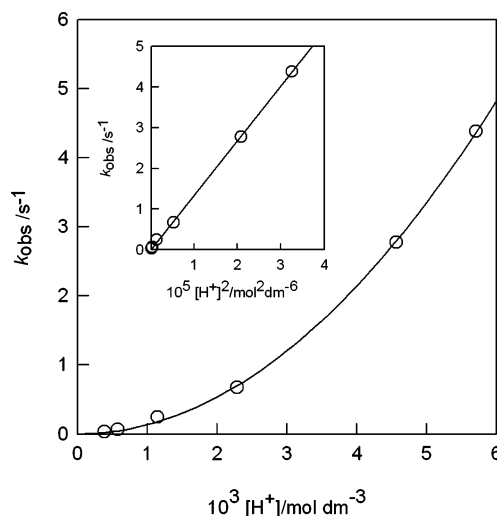

Figure 6. Plot of the observed rate constant for the reaction of [**1**]⁺ with HBF₄ in neat CH₃CN at 25.0 °C (0.1 mol dm⁻³ Et₄NBF₄).

fragment to the W₃S₄ core, the W−H electron density in [**1**]⁺ is lower than in the trinuclear cluster precursor, [W₃S₄H₃(dmpe)₃]⁺.

Because no reaction was observed in acetonitrile solution using [**1**][PF₆] and HCl, the stronger acid HBF₄ was used to obtain information about the kinetics of proton transfer in this solvent, and significant spectral changes were then observed. The kinetic study revealed that the reaction of [**1**]⁺ with HBF₄ in CH₃CN (0.10 mol dm⁻³ Et₄NBF₄) occurs in a single step, with observed rate constants k_{obs} that show a second-order dependence on the concentration of acid (eq 4, Figure 6) with a value of $k_{HBF4} = (1.34 \pm 0.01) \times 10^5$ dm⁶ mol⁻² s⁻¹. Interestingly, the final UV−vis spectrum observed for the reaction with HBF₄ matches that of intermediate **I₁** obtained by reacting [**1**]⁺ with HCl. As BF₄⁻ coordination appears unlikely and the spectrum of this species is independent of both the nature of the acid and the presence of H₂O in the solvent, the most likely formulation for **I₁** is [W₃PdS₄(CH₃CN)₃(dmpe)₃(CO)]⁴⁺. Unfortunately, attempts to study the kinetics of the reaction with HBF₄ in CH₃CN−H₂O (1:1) mixtures yield complex spectral changes that

suggest the existence of fluoride-abstraction processes, as previously observed for $[W_3S_4H_3(dmpe)_3]^+$.[17] To avoid that problem, HBF$_4$ was substituted by Hpts, and the supporting electrolyte was changed to Lipts. The reaction of $[1]^+$ with an excess of Hpts occurs with spectral changes that can be fitted by a single exponential both in neat CH$_3$CN and CH$_3$CN−H$_2$O (1:1) mixtures. The spectrum of the reaction product in both solvents is identical and matches within experimental error with that found for the reaction product with HBF$_4$ supporting the formulation of $\mathbf{I}_1$ as $[W_3PdS_4(CH_3CN)_3(dmpe)_3(CO)]^{4+}$. The values of the observed rate constants with Hpts in both solvents show a first-order dependence with respect to the acid (see the Supporting Information), with second-order rate constants of $(3.4 \pm 0.1) \times 10^3$ dm^{3}mol^{-1} s^{-1} in neat CH$_3$CN and 6.6 ± 0.1 dm^{3}mol^{-1} s^{-1} in CH$_3$CN−H$_2$O mixtures. The latter value compares well with that derived for the first step in the reaction with HCl, confirming that this step is kinetically controlled by proton attack on the cluster. In contrast, in neat CH$_3$CN, both the rate constant and the rate law change when the acid is changed from HBF$_4$ to Hpts, which adds further support to previous proposals stating that (H$^+$, X$^-$) ion pairs play an active role in the protonation of metal hydrides in aprotic solvents.[32,33]

$$k_{obs} = k_{HBF4}[H^+]^2 \qquad (4)$$

To confirm the formulation of the reaction product between $[1]^+$ and HBF$_4$ in CH$_3$CN ($\mathbf{I}_1$) as $[W_3PdS_4(CH_3CN)_3(dmpe)_3(CO)]^{4+}$, we monitored the process using multinuclear ^{1}H and ^{31}P{^{1}H} NMR and ESI-MS techniques. For this purpose, different aliquots of a solution of HBF$_4$ were added to a solution of $[1][PF_6]$, and the NMR spectra were recorded after each addition. Through the adequate selection of the amount of acid added, it is possible to detect the NMR signals of the intermediates formed between the starting reagent and the final product. These NMR experiments showed the sequential formation of two intermediates containing two and one W−H bonds and a final product that does not contain any of these bonds. The signals for the hydride and phosphorus atoms of the intermediate with two W−H bonds appear at $\delta_H = -1.62$ ($^2J_{H,P} = 46.2$ and 28.2 Hz) and -1.98 ($^2J_{H,P} = 49.4$ and 28.6 Hz), and $\delta_P = 2.86$, 0.91, -1.89, -2.84, -6.28, and -13.71. The signals for the intermediate with one W−H bond appear at $\delta_H = -1.61$ ($^2J_{H,P} = 51.9$ and 27.8 Hz) and $\delta_P = 3.50$, 1.33, -0.50, -2.69, -5.41, and -8.49, whereas for the final product, $\delta_P = 1.47$ and 0.17 and there are no hydride signals. The phosphorus spectra of both intermediates show six signals, because reaction at only one or two W−H bonds makes the dmpe ligands at different metal centers nonequivalent. Nevertheless, the symmetry is recovered when reaction occurs at the third metal center, so only two signals are observed again. These NMR results indicate that the single step observed in the

kinetic experiments actually corresponds to a process that occurs sequentially at the three metal centers with statistically controlled kinetics. In that case, the experimental kinetic traces yield only the observed rate constant for the reaction at the third metal center, although the rate constants for reaction at the three metal centers can be easily derived because they are in a 3:2:1 ratio.[18] It is interesting to note that the kinetics of the reaction of the incomplete cluster $[W_3S_4H_3(dmpe)_3]^+$ with acids was also found to be statistically controlled in neat CH$_3$CN and CH$_3$CN−H$_2$O mixtures,[17] although significant deviations from the statistical predictions were observed in CH$_2$Cl$_2$ solution.[18]

Attempts to prepare and isolate the hypothetical species $[W_3PdS_4(CH_3CN)_3(dmpe)_3(CO)]^{4+}$ were carried out by reacting the hydride cluster $[1]^+$ in acetonitrile with an excess of aqueous HBF$_4$. After precipitation with diethyl ether, a brown solid was obtained. Multinuclear NMR spectra of this solid dissolved in acetone-d_6 share common features with those recorded for the $[1][PF_6]$ and $[2][PF_6]$ clusters. In particular, two phosphorus signals are observed in the ^{31}P{^{1}H} spectra, and the characteristic four doublets pattern (due to the four methyl groups of each diphosphine) is observed in the ^{1}H spectra. Additionally, the ^{1}H spectra reveal the presence of one singlet at 1.9 ppm with an intensity similar to that of the methyl groups; the singlet is assigned to the coordinated acetonitrile. ^{1}H-^{3}C gHSQC experiments further confirm the presence of coordinated acetonitrile (coordinated CH$_3$CN signal at 12 ppm). This spectrum is given as Supporting Information, together with the spectra of $[1][PF_6]$ and $[2][PF_6]$, for comparative purposes. Although NMR spectroscopy provides enough evidence of the presence of $[W_3PdS_4(CH_3CN)_3(dmpe)_3(CO)]^{4+}$ in solution, it has to be pointed out that this species decomposes in acetone, acetonitrile, or dichloromethane solutions in a period of approximately 2 h. All attempts aimed to either obtain this species in analytically pure form or grow single crystals were unsuccessful.

Further support regarding the coordination of CH$_3$CN into the hydride sites of $[1]^+$ in acidic media, i.e., HBF$_4$, has been extracted though an ESI-MS analysis of $[1][PF_6]$ solutions in CH$_3$CN at different acid concentrations. The mass spectra clearly showed the presence of coordinated CH$_3$CN for the first reaction intermediate with a signal centered at 653 amu that is assigned to the $[W_3PdS_4H_2(CH_3CN)(dmpe)_3(CO)]^{2+}$ dication. This signal coexists with another one centered at 633 that can be assigned to the product resulting from the CH$_3$CN dissociation, namely $[W_3PdS_4H_2(dmpe)_3(CO)]^{2+}$ with a vacant coordination site (see Figure 7). On the basis of the NMR results, which indicate the existence of a single species with two coordinated hydrides, the most likely explanation is to assume that CH$_3$CN dissociation occurs during the mass spectra recording, although the existence of some degree of dissociation in the reaction mixture cannot be definitely ruled out.

The mass spectra recorded at higher HBF$_4$ concentrations show a signal centered at 449 that can be assigned to the intermediate with two coordinated acetonitrile molecules of formula $[W_3PdS_4H(CH_3CN)_2(dmpe)_3(CO)]^{3+}$. Unfortunately,

(32) Basallote, M. G.; Duran, J.; Fernandez-Trujillo, M. J.; Manez, M. A.; Rodriguez de la Torre, J. *J. Chem. Soc., Dalton Trans.* **1998**, 745.

(33) Basallote, M. G.; Duran, J.; Fernandez-Trujillo, M. J.; Manez, M. A. *Inorg. Chem.* **1999**, *38*, 5067.
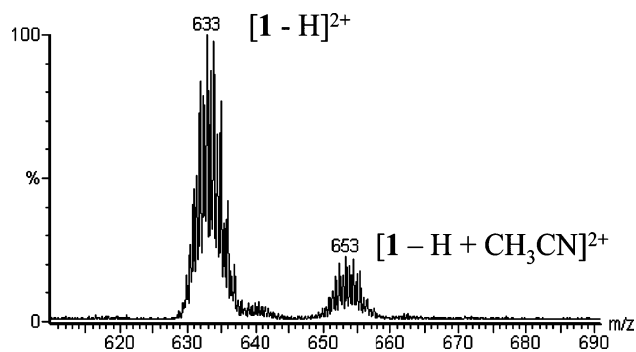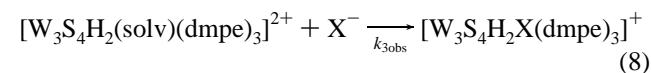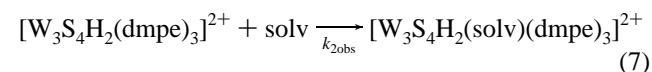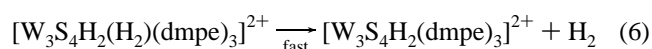
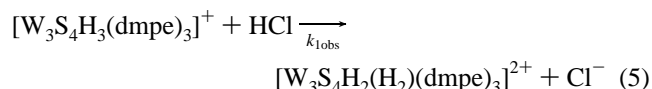**Figure 7.** ESI-MS spectra recorded after the addition of 1 equiv of HBF_4 to a solution of compound $[W_3PdS_4H_3(dmpe)_3(CO)][BPh_4]$ ($[1][BPh_4]$) in acetonitrile.

the MS experiments did not allow for the detection of the final $[W_3PdS_4(CH_3CN)_3(dmpe)_3(CO)]^{4+}$ product because of the high charge of the cluster.
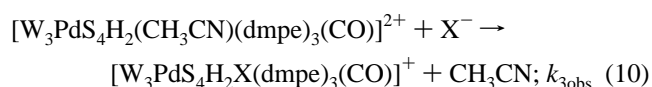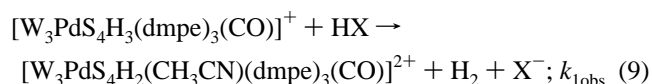
Mechanism of the Reaction of $[1]^+$ with Acids. The experimental information available for the reaction in eq 1 in CH_3CN and CH_3CN-water solution indicates that its mechanism must be rather similar to that proposed for the homometallic cluster precursor $[W_3S_4H_3(dmpe)_3]^+$, which has an incomplete cuboidal structure that lacks the Pd(CO) unit. For the reaction of the incomplete cluster, the acid-promoted substitution of the coordinated hydrides by Cl^- was explained in terms of the mechanism in eqs 5–8,[17] in which the initial attack by the acid to the W–H bond yields an unstable dihydrogen complex (eq 5) that rapidly releases H_2 and forms a coordinatively unsaturated complex (eq 6). This complex adds water in the next step (eq 7); finally, the coordinated water is substituted by the Cl^- anion (eq 8). Although, for simplicity, eqs 5–8 have been written showing the reaction at a single metal center, all these processes actually occur sequentially at each one of the three W–H bonds with statistically controlled kinetics.

$$[W_3S_4H_3(dmpe)_3]^+ + HCl \xrightarrow{k_{1obs}}$$
$$[W_3S_4H_2(H_2)(dmpe)_3]^{2+} + Cl^- \quad (5)$$

$$[W_3S_4H_2(H_2)(dmpe)_3]^{2+} \xrightarrow{fast} [W_3S_4H_2(dmpe)_3]^{2+} + H_2 \quad (6)$$

$$[W_3S_4H_2(dmpe)_3]^{2+} + solv \xrightarrow{k_{2obs}} [W_3S_4H_2(solv)(dmpe)_3]^{2+} \quad (7)$$

$$[W_3S_4H_2(solv)(dmpe)_3]^{2+} + X^- \xrightarrow{k_{3obs}} [W_3S_4H_2X(dmpe)_3]^+ \quad (8)$$

However, recent theoretical calculations have revealed that the formation of solvent adducts such as $[W_3PdS_4(CH_3CN)_3(dmpe)_3(CO)]^{4+}$ (I_1) is favored in front of dihydrogen complexes and/or coordinatively unsaturated species (eqs 5 and 6) and that proton attack on trinuclear cluster hydrides occurs through the diffusion-controlled initial formation of W–H···HCl dihydrogen-bonded adducts.[18] Acetonitrile attack on the W–H···HCl dihydrogen-bonded species produces the I_1 intermediate. The observation of intermediate I_1 from the reactions of cluster $[1]^+$ with HBF_4 and Hpts in CH_3CN also supports this interpretation. In this context, the

absence of a reaction between $[1]^+$ and HCl in neat CH_3CN is quite surprising. This can be explained by taking into account the nature of the protonating species; for the reaction with HCl in neat CH_3CN, the protonating species would be the HCl molecule itself, whereas for the other reactions, this is H^+_{solv}. Apparently, the energy cost associated with the rupture of the H–Cl bond makes the reaction in pure CH_3CN unfavorable for cluster $[1]^+$, in contrast with the hydride substitution observed for $[W_3S_4H_3(dmpe)_3]^+$ under analogous conditions.

Once the nature of I_1 has been established as the cluster resulting from a formal substitution of the hydride ligands by acetonitrile molecules, namely $[W_3PdS_4(CH_3CN)_3(dmpe)_3(CO)]^{4+}$, the unknown factor that remains for a satisfactory mechanistic interpretation of the acid-assisted substitution of the coordinated hydrides in $[1]^+$ is the determination of the nature of the intermediate I_2, which should be a cluster species halfway between complexes containing W–NCCH₃ and W–Cl bonds. In the case of the incomplete cluster $[W_3S_4H_3(dmpe)_3]^+$, the preparation of the trihydroxo complex $[W_3S_4(OH)_3(dmpe)_3]^+$ allowed for kinetic and NMR experiments that led to the formulation of I_2 as $[W_3S_4(H_2O)_3(dmpe)_3]^{4+}$.[17] However, in the present case, the observation of a single step in the reaction of $[1]^+$ with Hpts in a CH_3CN-H_2O mixtures introduces a serious argument against the formulation of I_2 as an aqua complex because, under those conditions, the reaction stops at the $[W_3PdS_4(CH_3CN)_3(dmpe)_3(CO)]^{4+}$ complex despite the large water excess. Given the fact that absorbance changes associated with the conversion of I_1 to I_2 are small and limited to a short wavelength range, we consider the interpretation that these absorbance changes correspond to some unknown secondary process and that the acid-promoted substitution of the coordinated hydrides in $[1]^+$ actually occurs in two kinetic steps to be a more-plausible interpretation. The first step is represented by eq 9, and the second one would consist of the substitution of CH_3CN by Cl^- with rate constants given by k_{3obs} (eq 10).

$$[W_3PdS_4H_3(dmpe)_3(CO)]^+ + HX \rightarrow$$
$$[W_3PdS_4H_2(CH_3CN)(dmpe)_3(CO)]^{2+} + H_2 + X^-; k_{1obs} \quad (9)$$

$$[W_3PdS_4H_2(CH_3CN)(dmpe)_3(CO)]^{2+} + X^- \rightarrow$$
$$[W_3PdS_4H_2X(dmpe)_3(CO)]^+ + CH_3CN; k_{3obs} \quad (10)$$

The kinetic results obtained for the initial protonation of the coordinated hydrides in cluster $[1]^+$ deserve some additional comment. There is recent evidence on the existence of competitive first- and second-order pathways for the protonation of the coordinated hydrides in $[W_3S_4H_3(dmpe)_3]^{+}$.[18] The second-order pathway requires two molecules of acid that assist the proton transfer by forming a M–H···H–X···H–X adduct with a shorter H···H distance, which facilitates the subsequent release of H_2. The operation of a second-order mechanism for the proton transfer in other transition-metal hydrides has been associated with the stabilization that results from the formation of homoconjugated HX_2^- species that require the presence of a second

acid molecule.[34,35] As HBF$_4$ does not exist in molecular form, the kinetics results found in the present work for the reaction of [**1**]$^+$ with HBF$_4$ in CH$_3$CN (eq 4) demonstrate that operation of the second-order pathway does not require a molecular acid able to form homoconjugated species or a solvent with a low dielectric constant, which indicates that the formation of the homoconjugated HX$_2^-$ species does not play a substantial role in the protonation of these clusters. In the case of these W$_3$S$_4$ or W$_3$PdS$_4$ cluster hydrides, the role of the second equivalent of acid in the second-order pathway seems to be mainly related to the formation of a network of hydrogen bonds that prepare the system for H$_2$ release.[18] We are currently carrying out both theoretical calculations and kinetic work on the reaction of [**1**]$^+$ with acids in dichloromethane solution in an attempt to gain new insights into the effects caused by the introduction of the Pd(CO) subunit into the different mechanistic pathways for the proton transfer to the coordinated hydrides.

As a summary, the results in the present work demonstrate that incorporation of Pd into the [W$_3$S$_4$H$_3$(dmpe)$_3$]$^+$ cluster produces air-stable heterodimetallic cubane type hydrido clusters in high yields. Whereas the W−H bonds in these W$_3$PdS$_4$ complexes show a reactivity similar to that found for the trinuclear hydride precursor, insertion of the heterometal modulates both the thermodynamics and the kinetics of the proton-transfer reaction at the W−H centers. In particular, there is an unexpected basicity decrease in the hydride ligands despite the electron-donating character found for the Pd(CO) fragment, which suggests an extensive reorganization of the electron density upon heterometal insertion that is also reflected in a significant expansion of the sulfur tetrahedron within the W$_3$PdS$_4$ core. However, for those thermodynamically favored processes, the kinetic data available indicate that the reaction mechanism is quite similar to that observed for the incomplete trinuclear cluster, with only small variations in the rate constants.

Supporting Information Available: X-ray crystallographic information in CIF format; plots of the dependence of the observed rate constant with the concentration of Hpts in acetonitrile (Figure S1) and acetonitrile−water (Figure S2) solution; and ^{1}H−^{13}C gHSQC spectra for compounds [**1**][PF$_6$] (Figure S3), [**2**][PF$_6$] (Figure S4), and species [W$_3$PdS$_4$(CH$_3$CN)$_3$(dmpe)$_3$(CO)]-[PF$_6$]$_x$[BF$_4$]$_{x-4}$ (Figure S5). This material is available free of charge via the Internet at http://pubs.acs.org.

IC052184U

(34) Papish, E. T.; Rix, F. C.; Spetseris, N.; Norton, J. A.; Williams, R. D. *J. Am. Chem. Soc.* **2000**, *122*, 12235.

(35) Belkova, N. V.; Besora, M.; Epstein, L. M.; Lledós, A.; Maseras, F.; Shubina, E. S. *J. Am. Chem. Soc.* **2003**, *125*, 7715.